



Article

Assessment of an Alternative Climate Product for Hydrological Modeling: A Case Study of the Danjiang River Basin, China

Yiwei Guo ^{1,2} , Wenfeng Ding ^{1,2,*}, Wentao Xu ^{1,2}, Xiudi Zhu ³, Xiekang Wang ⁴  and Wenjian Tang ^{1,2}

¹ Changjiang River Scientific Research Institute, Changjiang Water Resource Commission, Wuhan 430010, China; guoyiwei32ww@gmail.com (Y.G.); xuwt@mail.crsri.cn (W.X.); tangwj@mail.crsri.cn (W.T.)

² Research Center on Mountain Torrent Geological Disaster Prevention of Ministry of Water Resources, Wuhan 430010, China

³ Changjiang Water Resources Protection Institute, Wuhan 430051, China; zhuxiudi@mail.bnu.edu.cn

⁴ State Key Laboratory of Hydraulics and Mountain River Engineering, Sichuan University, Chengdu 610065, China; wangxiekang@scu.edu.cn

* Correspondence: dingwf@mail.crsri.cn; Tel.: +86-189-7168-9795

Abstract: Precipitation has been recognized as the most critical meteorological parameter in hydrological studies. Recent developments in space technology provide cost-effective alternative ground-based observations to simulate the hydrological process. Here, this paper aims to evaluate the performance of satellite-based datasets in the hydrological modeling of a sensitive area in terms of water quality and safety watershed. Three precipitation products, i.e., rain gauge observations (RO), the China Meteorological Assimilation Driving Datasets for the SWAT model (CMADS), and Tropical Rainfall Measuring Mission Multi-satellite (TRMM) products, were used to develop the Soil and Water Assessment Tool (SWAT) model to simulate the streamflow in the Danjiang River Basin (DRB). The results show that: (1) these three precipitation products have a similar performance with regard to monthly time scale compared with the daily scale; (2) CMADS and TRMM performed better than RO in the runoff simulations. CMADS is a more accurate dataset when combined with satellite-based and ground-based data; (3) the results indicate that the CMADS dataset provides reliable results on both monthly and daily scales, and CMADS is a possible alternative climate product for developing a SWAT model for the DRB. This study is expected to serve as a reference for choosing the precipitation products for watersheds similar to DRB where the rain gauge data are limited.

Keywords: SWAT; CMADS; TRMM; the Danjiang river basin



Citation: Guo, Y.; Ding, W.; Xu, W.; Zhu, X.; Wang, X.; Tang, W. Assessment of an Alternative Climate Product for Hydrological Modeling: A Case Study of the Danjiang River Basin, China. *Water* **2022**, *14*, 1105. <https://doi.org/10.3390/w14071105>

Academic Editor: Pankaj Kumar

Received: 14 March 2022

Accepted: 29 March 2022

Published: 30 March 2022

Publisher's Note: MDPI stays neutral with regard to jurisdictional claims in published maps and institutional affiliations.



Copyright: © 2022 by the authors. Licensee MDPI, Basel, Switzerland. This article is an open access article distributed under the terms and conditions of the Creative Commons Attribution (CC BY) license (<https://creativecommons.org/licenses/by/4.0/>).

1. Introduction

Precipitation has been recognized as the most critical meteorological parameter in relation to developing hydrological models, because its spatiotemporal variability has a significant impact on hydrological behavior and water distribution [1–3]. Previous research studies have illustrated that having less precipitation information uncertainty has a sizable effect on stabilizing model parameterization and calibration [4–6]. However, there are severe limitations to describing rainfall inputs' true spatiotemporal variability of a river basin accurately, such as the rainfall pattern influenced by the complex topography and impacted by a hierarchy of regionally dominated atmospheric cycles [7,8].

Precipitation observed from a rain gauge, in general, is considered to be actual rainfall [9,10]. In most cases, point rainfall measurements are spatially interpolated to illustrate the rainfall field at a basin scale, and hence they are used as inputs in spatial-distributed hydrological models [11,12]. Field rainfall obtained from such interpolation, however, can represent the true distribution of precipitation well only if the rain gauges are deployed with reasonable density and uniform distribution [13]. Unfortunately, in most areas, especially in remote and developing areas, rain gauges are distributed irregularly

and sparsely [14–17]. Consequently, the true rainfall field is poorly represented through interpolation, challenging the application of hydrological models. The accidental missing of the ground observations also exacerbate this challenge [18,19].

Recently, the feasibility of satellite-based data as alternatives for describing the temporal and spatial variability of the true rainfall field has been frequently tested. For example, Hur et al. [20] compared two high-resolution satellite rainfall datasets (TRMM 3B42 v7.0 and GSMaP v5.222) with rain gauge observations in Singapore. It was found that TRMM 3B42 v7.0 and GSMaP v5.222 both tended to overestimate the light rain and frequency but underestimate high-intensity precipitation when extreme precipitation was analyzed. Jiang et al. [21] researched a middle-latitude basin in South China, pointing out that rainfall was overall largely underestimated when using TMPA 3B42RT, Precipitation Estimation from Remote Sensing Information using Artificial Neural Network (PERSIAN), and the NOAA/Climate Precipitation Center Morphing Technique (CMORPH). Duncan et al. [22] assessed the accuracy of satellite-derived precipitation estimation (TRMM) over Nepal and found that though the precipitation of TRMM was significantly correlated with ground-based observations in all seasons, satellite precipitation estimates consistently overestimated the amount of precipitation and inaccurately detected extreme precipitation events.

The distributed hydrological model is beneficial for understanding the hydrological process [23–25]. The most habitually utilized distributed hydrological models have been appeared to effectively consolidate information from rain gauges, whereas satellite-based precipitation has been persistently moved forward and integrated into distinctive modules that assess its execution in simulating watershed streamflow [26,27]. The Soil and Water Assessment Tool (SWAT) is the most widely used distributed hydrological model among all the various hydrological models [28–31]. Huang et al.'s [32] study in the German state of Baden-Württemberg used three precipitation datasets with different time scales (daily, sub-daily, and diurnal) as inputs to drive a SWAT model to simulate the runoff, and found that there is a positive correlation between model performance and higher precipitation resolution. Yeganantham et al. [33] found that Climate Hazards Group InfraRed Rainfall with Station (CHIRPS) performed better than Climate Forecast System Reanalysis (CFSR) in simulating streamflow when using the SWAT model in ten watersheds located in the USA, Brazil, Spain, Ethiopia, and India. Hamoud et al.'s research [34] showed that the applicability of CHIRPS and TRMM 3B42 in runoff simulations were better than that of CFSR, Artificial Neural Networks–Climate Data Record (PERSIANN-CDR), and European Atmospheric Reanalysis (ERA-5) in the Highland Region of Yemen. Moreover, the performances of the satellite-based data are various in different areas. For example, Mararakanye et al.'s research in the lower Vaal River Catchment area (South Africa) [35] found that the CFSR performed well in simulating runoff by using a hydrological model, while according to Dao et al.'s study in the Cau River Basin (North Vietnam) [36], the performance of CFSR in runoff simulation was unsatisfactory. Gao et al. [37] proved that the performance of PERSIANN-CDR as an input to drive the SWAT model to simulate runoff was not suitable for the Xiang River Basin (China); however, its performance when simulating runoff was good in the Lancang River Basin (China). Like the studies above, the results simulated using the data-based SWAT model are heterogeneous and the performance of satellite-based datasets to simulate runoff should be evaluated for the specific basin.

Originating from the Q-DM, the Danjiang River Basin (DRB) is the main water source of the central route projects of the South-to-North Water Diversion Project [38]. This project is one of the most important hydraulic engineering projects in China and aims to improve the water shortage problem in northern China and improve the ecological environment along the related region. The quantity and quality of the water delivered are influenced by the erosion of the DRB [39,40]. Therefore, the DRB is considered to be a sensitive area in terms of water quality and safety with regard to the watershed. However, the uneven distribution of the meteorological stations in Q-DM makes it difficult to understand the real hydrological process. A previous study [41] used CFSR-driven SWAT models to simulate the runoff in the Bahe River Basin (Q-DM area) and found that the runoff simulated by

uncorrected CFSR data were only satisfactory in this basin, while corrected data performed better. This indicates that it is necessary to verify the applicability of meteorological data in the DRB (Q-DM area).

Here, this study explores the results of the CMADS, TRMM, and rain gauge data when simulating rainfall estimation and surface runoff at monthly and daily scales in the DRB. The study aims to verify the applicability of the CMADS data and TRMM data in the DRB, and it can, therefore, serve as a reference for choosing the precipitation datasets in watersheds similar to the DRB where the ground-based rain gauge data are unavailable. With the objectives above, this study involves (1) a comparison of rainfall estimations from CMADS, TRMM 3B42 data, and rain gauge observations (Gauge) at monthly, daily, and spatial scales, (2) setting up a SWAT model with CMADS, TRMM 3B42 data, and rain gauge observations to simulate monthly and daily runoff, (3) calibrating and validating the simulated streamflow at three hydrological stations using the SWAT Calibration Uncertainties Program (SWAT-CUP) which uses the Sequential Uncertainty Fitting ver.2 (SUFI-2) algorithm, and (4) evaluating the multi-statistical performance of the simulation against the observed streamflow data. The main goal of this study is to evaluate the use of satellite-based and reanalysis precipitation products as model operation driving data, and assess whether they can drive the model in a watershed similar to the DRB where the gauge observations are limited.

2. Materials and Methods

2.1. Study Area

The largest tributary of the Hanjiang River, the Danjiang River, is a mountain river that covers a drainage area of 8887 km². The total length of its main stream is 280 km. Originating from the South Qinling Mountains and flowing into the Hanjiang River [42], the Danjiang River flows through the Shaanxi, Henan, and Hubei Provinces. It stretches between 33°04'10" N and 34°11'09" N and across 109°30'08" E and 111°15'51" E. The Danjiang River Basin (DRB) features a high-rising west and a low-lying east, with a relative elevation difference of 1915 m. The continental monsoon climate contributes to the distinct seasons of the DRB. According to the records from 1950 to 2015, the long-term annual precipitation of the DRB is 732.29 mm and the spatial distribution difference shows an increasing trend from the west to the east. Rainfall is concentrated in the period from May to October, accounting for about 80% of the annual precipitation. Moreover, the annual average temperature ranges from 7.8 °C to 13.9 °C and the annual runoff is 14.36×10^8 m³.

Forestland occupies the largest area in the DRB, followed by the cropland. The yellow-brown soil and sandy loam are the dominant soil types in the DRB [38]. There are 3 hydrological stations (Majie Station upstream, Danfeng Station midstream, and Jingziguan Station downstream) and 58 ground-based rain gauges in the study area. The digital elevation model (DEM), stream network, weather stations, and hydrological stations are shown in Figure 1.

2.2. Hydrological Model and Data Sources

In this study, the SWAT model was used for hydrological modeling, which was developed by USDA-ARS. Because the SWAT model is designed for long-term simulations on a daily scale, it is suitable for evaluating the performance of three precipitation products. To ensure the accuracy of relative changes induced by different precipitation inputs, all input parameters, such as temperature, wind, solar radiation, and humidity, were kept the same, except precipitation. Additionally, the temperature, wind, solar radiation, and humidity inputs were simulated by the internal weather generator of SWAT.

Moreover, the target watershed is required by the SWAT model to be divided into sub-watersheds. Each sub-watershed may include one or more Hydrologic Response Units (HRUs). On the basis of the 30 m DEM and by choosing the Jingziguan Station as the outlet, the controlled watershed was delineated. The threshold to discretize the sub-watershed was based on the 2% area. Other input parameters, such as soil type and land use, were

downloaded from websites (Table 1). The data of measured runoff were obtained from the Department of Hydrology of the Ministry of Water Resources of China. Additionally, the SPWA (Soil–Plant–Air–Water) software was used to analyze the soil–water characteristics of each soil type.

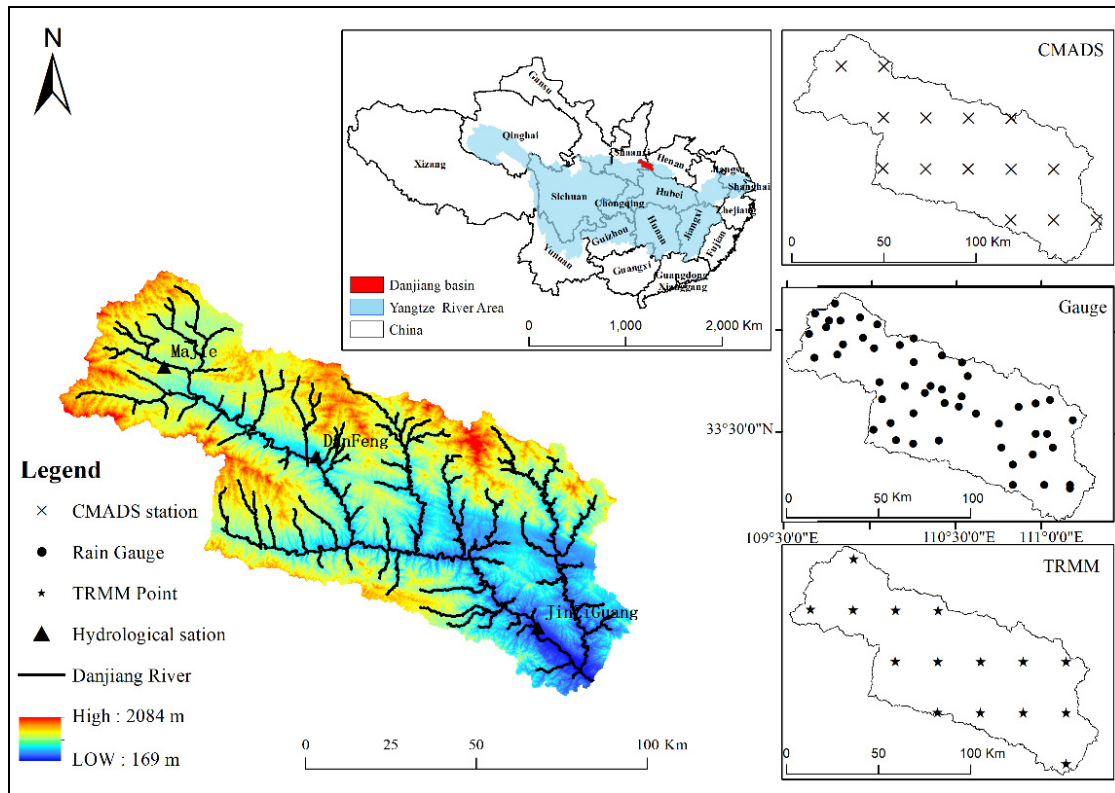


Figure 1. Location of the Danjiang River Basin and the distribution of hydrological stations, CMADS stations, TRMM points, and rain gauges.

Table 1. Summary of the input parameters.

Parameters	Dataset	Developed Organization	Resolution	Data Source (Accessed on 1 August 2021)
DEM	Shuttle Radar Topography Mission (SRTM)	National Aeronautics and Space Administration (NASA)	30 m	https://earthexplorer.usgs.gov/
Land cover	30 m-resolution Global Land Cover (GLC30)	The National Geomatics Center of China (NGCC)	30 m	http://www.globallandcover.com/
Soil type	World Soil Database (HWSD)	The Food and Agriculture Organization of the United Nations (FAO)	1000 m	http://www.fao.org/soils-portal/soil-survey/soil-maps-and-databases/harmonized-world-soil-database-v12/en/

Daily rainfall data were collected from weather gauge stations and the two satellite-based and reanalysis precipitation products used were CMADS and TRMM 3B42 version 7.

Daily precipitation data obtained from the fifty-eight rain gauges in the DRB were available from the website of the Department of Hydrology of the Ministry of Water Resources of China. The rain gauge data covered from 1964 to 2015.

The dataset CMADS introduces the technology of The Space and Time Mesoscale Analysis System (STMAS) assimilation algorithm. Multiple technologies and scientific methods were used to develop CMADS [43,44]. The dataset, containing information relating to precipitation, temperature, and other variables, can be used to run hydrological models such as SWAT. The precipitation data of CMADS are merged with the hourly precipitation data collected by the China National Meteorological Information Center using the CPC MORPHing technique (CMORPH). CMADS stations provide information throughout the day from 2008 to 2016 in the areas between 0–65° N and 60–160° E. There are a total of 19 CMADS stations in the study area.

In late 1997, the TRMM satellite was launched by the National Aeronautics and Space Administration (NASA) and the Japanese Aerospace Exploration Agency (JAXA) to monitor precipitation [45]. TRMM 3B42 is one of the RMM Multi-satellite Precipitation Analysis (TMPA) products [46]. It provides daily precipitation data from 50° S to 50° N at a resolution of 0.25° spatially and temporally from 1998 to 2015 [47,48]. There is a total of 19 TRMM 3B42 pixels in the study area. Further information about TRMM and CMADS can be found in Table 2.

Table 2. Summary of remote-sensing/reanalysis precipitation datasets.

Full Name	Abbreviation	Coverage	Spatiotemporal Resolution Used	Data Source (Accessed on 1 August 2021)
The China Meteorological Assimilation Driving Datasets for the SWAT model Version 1.1	CMADS V1.1	0–65° N 60–160° E	Daily, 0.25°	http://www.cmads.org/
Tropical Rainfall Measuring Mission Multi-satellite Precipitation Analysis 3B42 Version 7	TRMM 3B42 V7	50° S–50° N	Daily, 0.25°	https://disc.gsfc.nasa.gov/

The SWAT model uses data from the station nearest to the centroid of each sub-basin to categorize precipitation data into sub-basins [47].

2.3. Model Calibration and Evaluation

When all parameters were entered into the SWAT model, the SWAT model ran with three precipitation products (rain gauge data, CMADS dataset, and TRMM dataset) separately at the monthly and daily scale. The watershed was divided into a total of 237 sub-catchments by the SWAT model, and these sub-watersheds were further divided into 980 HRUs on the basis of the land use, soil type, and slope classes. The simulated period was selected to be the period from 2008 to 2015 to ensure its consistency, because the available gauge data, CMADS data, and TRMM data were, respectively, collected from 1964 to 2015, 2008 to 2018, and 1998 to 2015. Here, 2008 was taken as the warm-up period.

The SUFI-2 algorithm in SWAT-CUP was used in the calibration procedure. On the basis of Duan et al.'s research [48] and the official guide, 17 parameters were selected. Considering the influence of elevation on precipitation, the precipitation lapse rate (PLAPS) was introduced [49]. Moreover, the simulated results of the Majie Station, Danfeng Station, and Jingziguan Station were calibrated together. The model was calibrated by first using the initial value ranges of each parameter and then using the suggested ranges of the previous simulation. The simulations were calibrated five times with 500 iterations each.

In this study, the coefficient of determination, Nash–Sutcliffe efficiency (NSE), and percent bias (PBIAS) were used to evaluate the accuracy of runoff modeling results. The formulas are as follows [35]:

$$R^2 = \left(\frac{\sum_{i=1}^n (Q_i - \bar{Q}_i)(S_i - \bar{S}_i)}{\sqrt{\sum_{i=1}^n (Q_i - \bar{Q}_i)^2} \sqrt{\sum_{i=1}^n (S_i - \bar{S}_i)^2}} \right) \quad (1)$$

$$NSE = \frac{\sum_{i=1}^n (S_i - Q_i)^2}{\sum_{i=1}^n (Q_i - \bar{Q}_i)^2} \quad (2)$$

$$PBIAS = \frac{\sum_{i=1}^n (S_i - Q_i)}{\sum_{i=1}^n Q_i} \times 100\% \quad (3)$$

where Q_i is the observed value, S_i is the simulated value, and \bar{Q}_i and \bar{S}_i are the mean values of the observed and simulated values. The statistical threshold values that were used to evaluate the performance of the model are shown in Table 3.

Table 3. The statistical threshold values used for interpreting model performance.

Performance Ratings	R ²	NSE	PBIAS
Very Good	0.7~1	0.75~1	<±10
Good	0.6~0.7	0.65~0.75	±10~±15
Satisfactory	0.5~0.6	0.50~0.65	±15~±25
Unsatisfactory	≤0.5	≤0.5	≥±25

3. Results

3.1. Evaluation of the Three Precipitation Products

3.1.1. Monthly Scale

The comparison of the SWAT model results using the three precipitation products from 2009 to 2015 in the study area is shown in Figure 2. The dry (drought), wet (rainy), and normal years were defined on the basis of the commonly used precipitation year classification standard [50]. In this study, 2010, 2013, and 2015 were denoted as drought years and 2009, 2011, and 2012 were denoted as rainy years. It is noted from Figure 2 that the annual rainfall mainly concentrates in the period from June to August (the flood season), and the precipitation calculated by the rain gauge, CMADS, and TRMM from June to August, respectively, account for 51.53%, 54.61%, and 54.60% of the annual precipitation. Figure 2 also shows that, before 2013, the CMADS and TRMM both underestimated the rainfall severely in the flood season of the rainy years compared with actual precipitation, by 32.51% and 11.66%, respectively, and that the CMADS and TRMM overestimated the rainfall by 18.12% and 40.48%, respectively, in the flood season of the drought years. The rainfall estimated by CMADS and TRMM was similar to the estimation of Gauge in non-flood seasons. The situation has improved since 2013. The precipitation trend of CMADS and Gauge became similar after 2013 because the underestimation of CMADS's precipitation was narrowed. However, TRMM still underestimated the rainfall in the flood season of rainy years and overestimated the rainfall in the flood season of normal years after 2013, though the precipitation deviation was reduced. In addition, the Pearson correlation coefficient of Gauge and CMADS (Gauge-CMADS) and Gauge and TRMM (Gauge-TRMM) were 0.74 and 0.75, respectively, indicating that the precipitation of CMADS and TRMM were highly similar to the precipitation of the rain gauges. In other words, the rainfall in this area can be effectively represented by CMADS and TRMM.

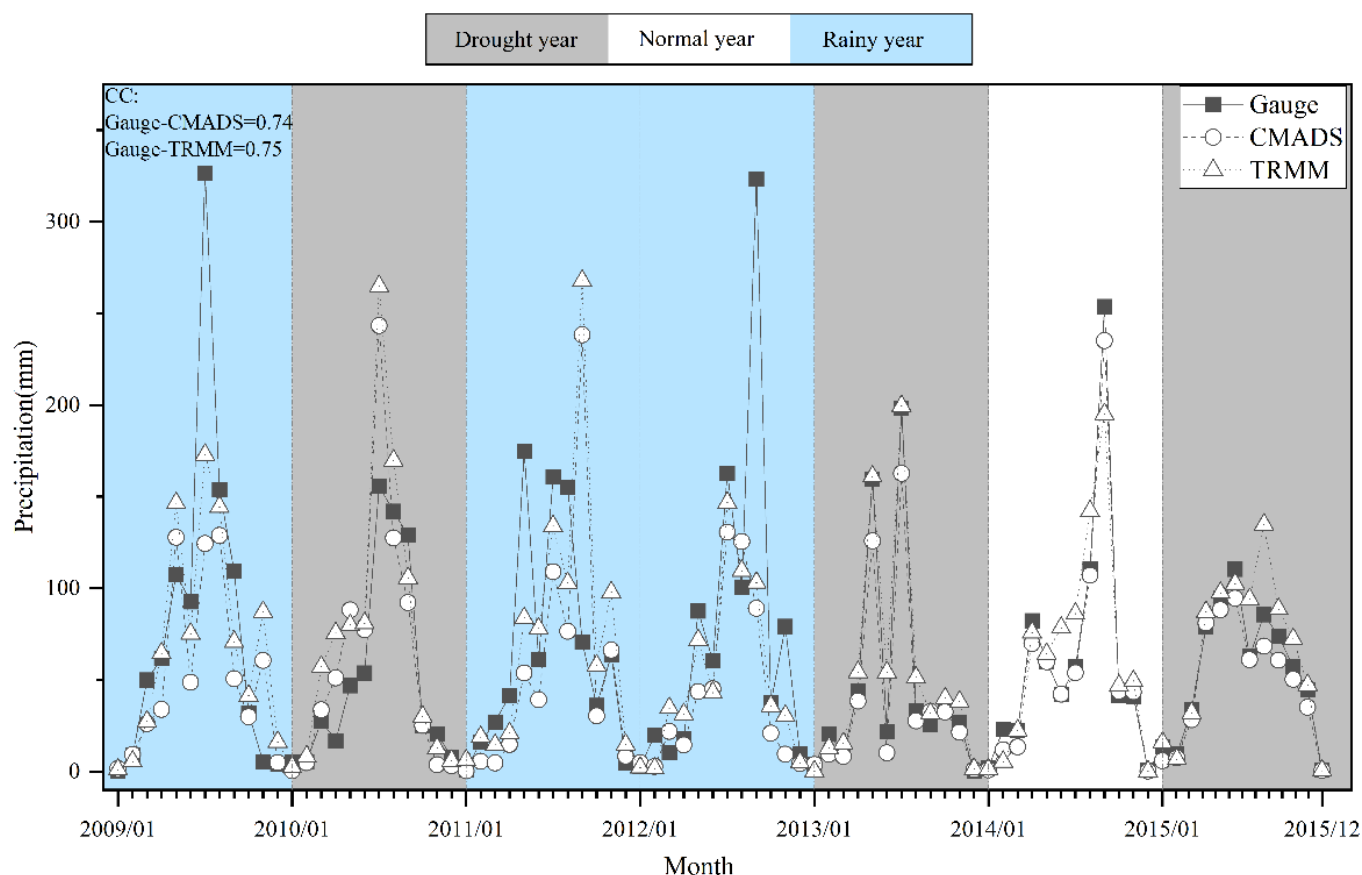


Figure 2. Three different precipitation records at monthly scale in the DRB (the CC value of Gauge-CMADS and Gauge-TRMM were 0.74 and 0.75, respectively; 2009, 2011, and 2012 were denoted as rainy years, 2014 was denoted as the normal year, and 2010, 2013, and 2015 were denoted as drought years. Additionally, the data in this figure were given as year and month.

It can be seen from the box plot of Figure 3 that the precipitation featured three peaks, with the peak values appearing in May, July, and September. The monthly precipitation of CMADS had the largest average and median line, while the average and median line of TRMM was the smallest. Moreover, CMADS reported the largest maximum rainfall except in October and December, and TRMM had the smallest minimum precipitation throughout the year. In addition, the PBIAS values of Gauge-CMADS and Gauge-TRMM were -18.86 and 3.20 , respectively, indicating that the CMADS precipitation was underestimated compared to the Gauge precipitation, with the TRMM estimation the exact opposite. However, the total precipitation was not much different. In summary, compared with the Gauge records, CMADS tends to overestimate the rainfall, while TRMM tends to underestimate the rainfall.

3.1.2. Daily Scale

The intensity and frequency of precipitation are the critical parameters used to describe the characteristic of daily rainfall [51]. It is noted from Figure 4 that the angle between the CMADS model's 95%-line estimates and the horizontal axis was $<45^\circ$ and that the angle between the TRMM model's 95%-line estimates and the horizontal axis was $<45^\circ$ as well. This suggested that although the precipitation trends of CMADS and TRMM were similar to that of the Gauge records at a daily scale, the CMADS and the TRMM rainfall data tended to be underestimated when extreme rainstorms occurred. The CMADS and the TRMM, respectively, underestimated the storm rainfall (>50 mm/day) by 13.11% and 10.65%, showing that the CMADS and TRMM were less capable of accurately simulating the storm rainfall than Gauge.

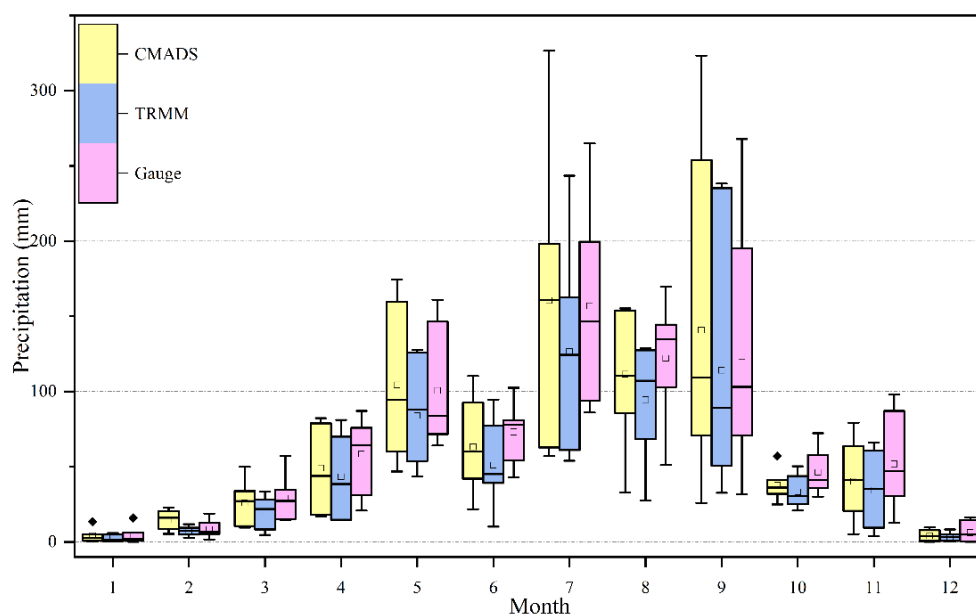


Figure 3. The box diagrams of three precipitation records at a monthly scale in the DRB.

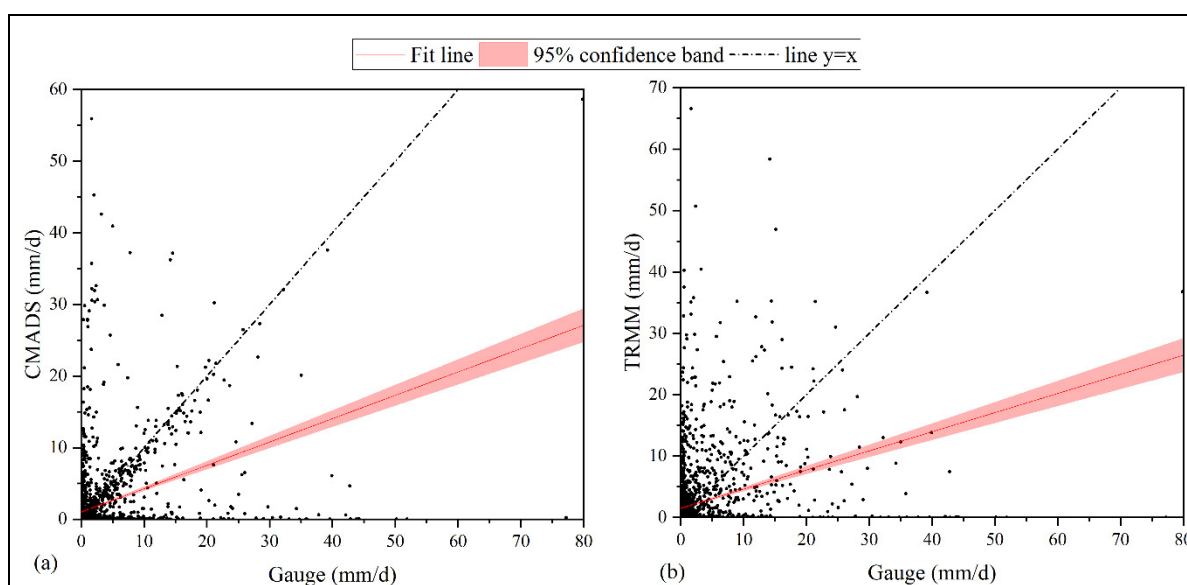


Figure 4. Scatterplot of the CMADS and TRMM records compared with Gauge records at a daily scale: (a) comparison of CMADS and Gauge and (b) comparisons of TRMM and Gauge. Note that the straight lines that pass through the origin are dividing lines with an angle of 45° to the x-axis, which means that the precipitation products overestimated the rainfall if the point is higher than this line.

Moreover, the Pearson correlation coefficients of Gauge-CMADS and Gauge-TRMM were 0.39 and 0.32, respectively, and the Pearson correlation coefficient of CMADS-TRMM was 0.80, indicating that there were big differences between Gauge and CMADS data and between Gauge and TRMM data, while the CMADS and TRMM data were similar.

The cumulative daily precipitation intensity frequencies of the three precipitation products are shown in Figure 5. Taking 50 mm/day as the panel line, Figure 5a was divided into Figure 5b,c to describe the frequency trend of the three precipitation products clearly. It can be noticed that the three products have the smallest difference in the events of less-than-heavy rain (30 mm/d), but the largest difference in the events of torrential rain (>50 mm/d). Additionally, the number of torrential rain events identified by TRMM was

lower than that in Gauge records, and the frequency of torrential rain identified by CMADS was the lowest among the three precipitation products.

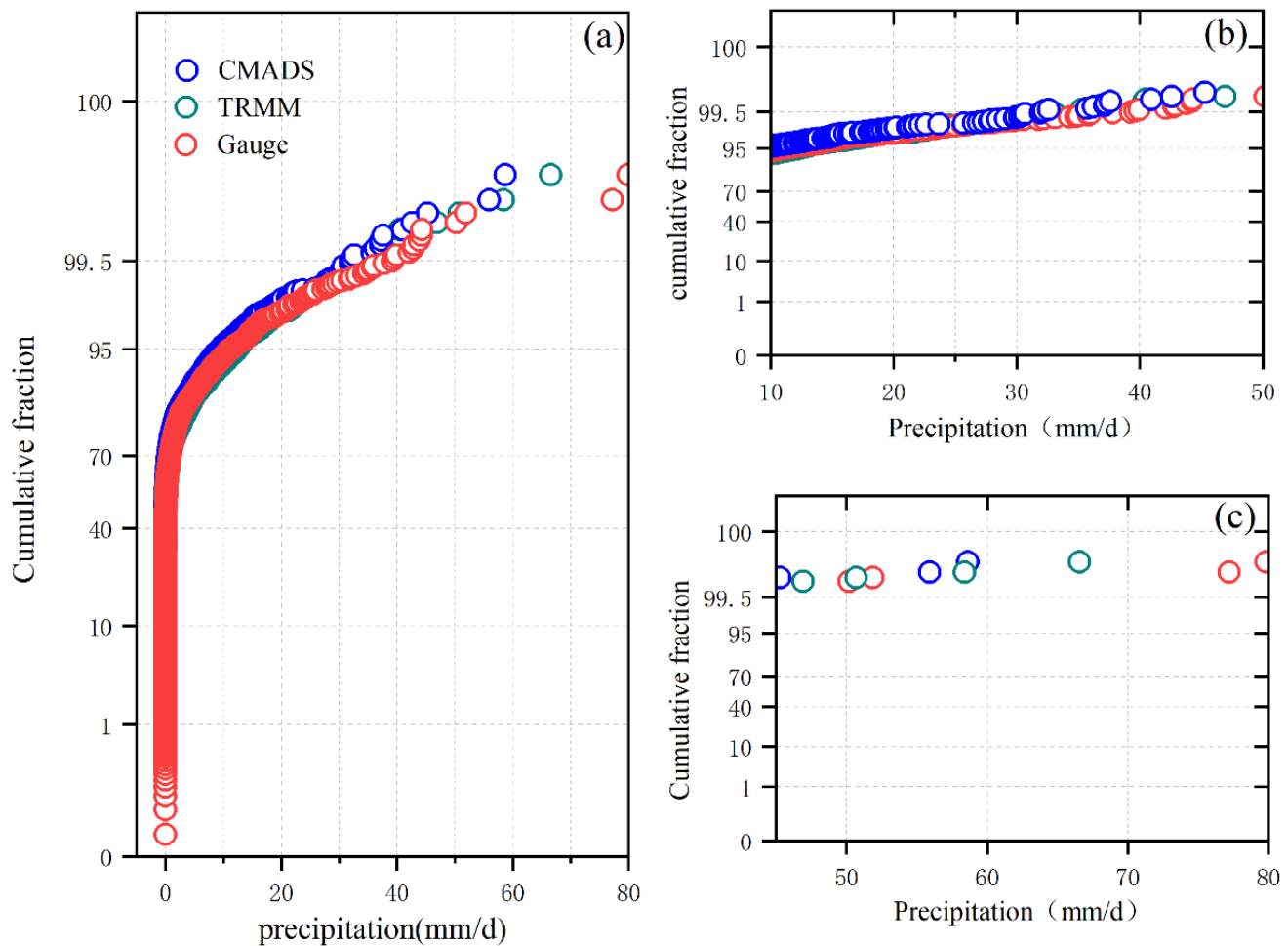


Figure 5. Cumulative frequencies of daily precipitation intensity for Gauge (red points), CMADS (blue points), and TRMM (green points) in the DRB: (a) distribution of all precipitation values, (b) distribution of precipitation values that are < 50 mm, and (c) distribution of precipitation values that are ≥ 50 mm.

3.1.3. Spatial Scale

The spatial distributions suggested by the three precipitation products were almost completely different, as shown in Figure 6. CMADS suggested that the rainfall increased from the center to the surroundings, with the highest rainfall in the central north. The clear trend of precipitation suggested by TRMM was that rainfall increased from upstream to downstream, with the highest rainfall in the east. However, the rainfall of Gauge in each sub-basin varied greatly, and there was no obvious spatial distribution pattern mainly due to the distribution of the rain gauge stations. Though there are a large number of rain gauge stations (58 stations) in the study area, most of them are located in the north and the east, leaving a vast area in the central west and southeast of the basin with no rainfall stations. Meanwhile, the CMADS (15 stations) and TRMM (15 stations) grid data were collected from uniformly distributed stations, causing the different spatial distribution of rainfall. Moreover, regardless of the daily or the monthly scale, the similarity of rainfall between CMADS and Gauge was higher than that of TRMM.

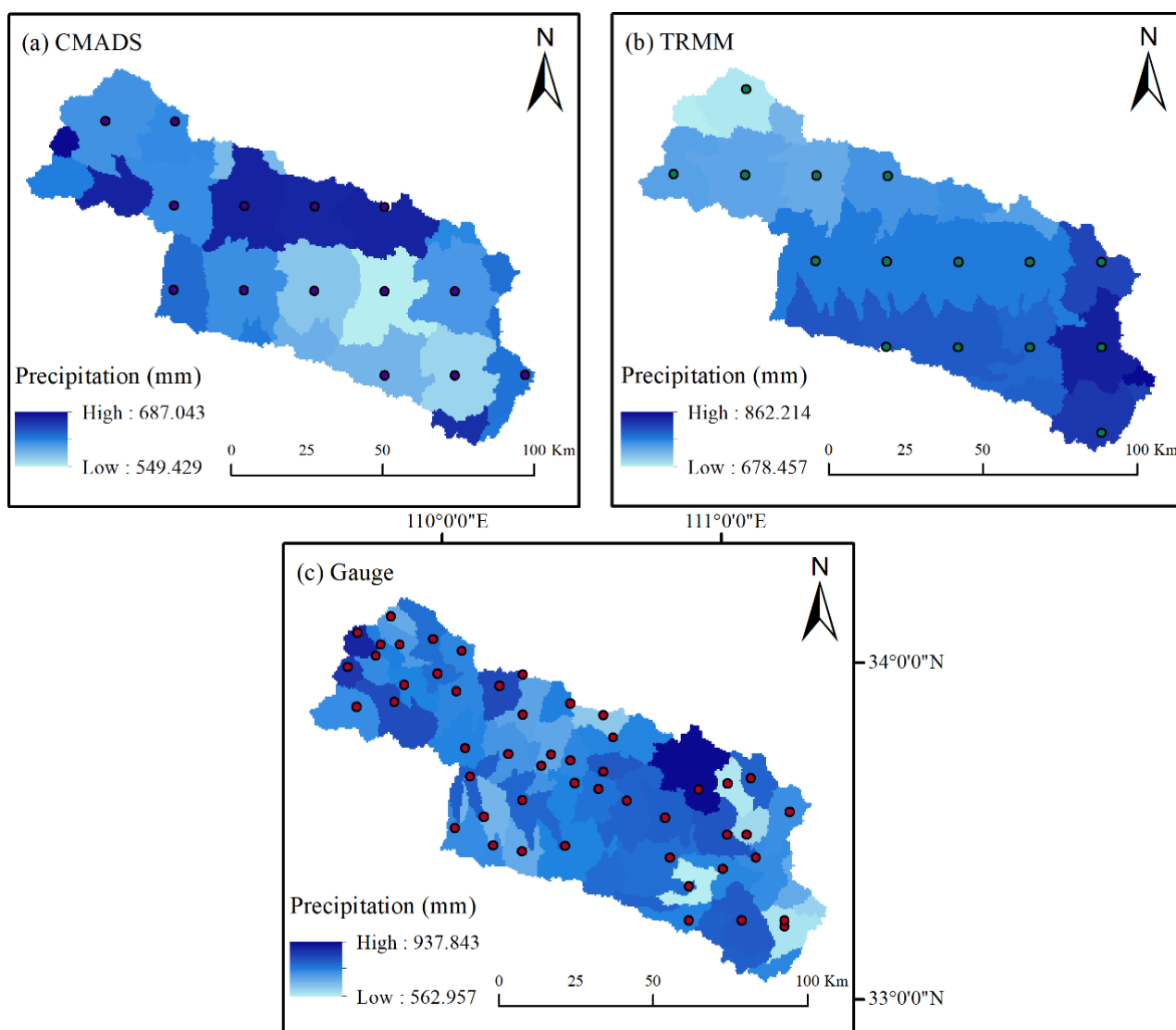


Figure 6. Spatial variation of precipitation at a yearly scale for all sub-basins calculated with precipitation inputs from (a) CMADS, (b) TRMM, and (c) Gauge.

Though the rainfall gauges are able to reflect more information than CMADS and TRMM when describing the variation of precipitation, the areal rainfall interpolated from the gauges may be distorted because the gauges' observations are point data. However, the CMADS and TRMM data are evenly distributed grid data with a resolution of 0.25° and reflect the areal rainfall. Thus, despite the better performance of the rain gauge data in describing watershed areal rainfall among three products, which products perform the best in driving SWAT model to simulate runoff is uncertain.

3.2. The Performance of Different Precipitation Products in Simulating Runoff

3.2.1. Pre-Calibration Model Results

Before the model was calibrated, we conducted a statistical analysis of the simulation results of runoff during the simulation period (2008–2015) of the model. As is shown in Table 4, the runoff simulation results of the three precipitation products downstream, midstream, and upstream showed different trends. The best simulation effect was upstream (Majie Station), while the worst performance was midstream (Danfeng Station). Moreover, the best simulation performance was achieved by CMADS, whose NSE was 0.74 upstream and 0.63 downstream (Jingziguan Station), while the worst simulation effect occurred in Gauge with its NSE almost all below zero (it was only above zero in the Majie Station).

Furthermore, the PBIAS values of the Gauge model were all below zero, showing that the simulation value of the Gauge model was smaller than the measured runoff. The PBIAS values of the CMADS model and TRMM model were both above zero upstream and below zero midstream and downstream, indicating that the simulation values of these two products were larger than the measured runoff in the upper stream and smaller than the actual runoff in the middle and downstream.

Table 4. The pre-calibration performance error amounts of the SWAT model simulated with CMADS, TRMM, and Gauge data on a monthly scale.

Station	R ²			NSE			PBIAS		
	CMADS	Gauge	TRMM	CMADS	Gauge	TRMM	CMADS	Gauge	TRMM
Majie Station	0.79	0.5	0.68	0.74	0.43	0.66	23.4	−22.38	10.44
Danfeng Station	0.04	0.05	0.05	−0.7	−1.52	−7.24	−7.67	−56.43	−32.1
Jingziguan Station	0.7	0.06	0.63	0.63	−0.82	0.51	−63.35	−164.97	−164.7

The pre-calibration results of the monthly scale indicated that the CMADS and TRMM data were reliable in estimating runoffs; the R² values of CMADS-SWAT and TRMM-SWAT were 0.79 and 0.68, respectively. Though the performance of Gauge-SWAT was not as good as CMADS-SWAT, it was still a valuable data source for use in the model, for its R² was 0.50.

It is noted from Table 5 that the simulation results of the three precipitation products on a daily scale showed the same trend as that on a monthly scale in the upper, middle, and lower reaches of the basin. The simulation performance in the upstream was the best and the performance downstream was the worst. Moreover, the NSE values of the CMADS model and the TRMM model were all below 0.6 in the entire basin, meaning that their performances were unsatisfactory. Additionally, the PBIAS values of the CMADS model were all above zero, the PBIAS values of the Gauge model were all below zero, and the PBIAS values of the TRMM model were above zero in the upstream and below zero in the midstream and downstream, indicating that the simulation values of the CMADS model and Gauge model were, respectively, higher and lower than the measured runoff in the whole basin and that the simulation value of TRMM model was higher in the upper reach but lower in the middle and lower reaches.

Table 5. The pre-calibration performance error amounts of the SWAT model simulated with CMADS, TRMM, and Gauge data on the daily scale.

Station	R ²			NSE			PBIAS		
	CMADS	Gauge	TRMM	CMADS	Gauge	TRMM	CMADS	Gauge	TRMM
Majie Station	0.39	0.18	0.22	0.38	0.11	0.18	22.98	−23.02	9.83
Danfeng Station	0.32	0.05	0.2	0.16	−1.24	−0.23	1.65	−47.57	−24.83
Jingziguan Station	0.26	0.02	0.16	0.25	−0.57	0.03	60.82	−160.86	−143

All these three datasets seriously overestimate the runoff in the middle stream and downstream, according to Figure 7B,C. Moreover, the average observed streamflow was smaller than the average simulated runoff throughout the year in the upstream, except in September. The mean standard deviation of the three precipitation products computed at the monthly time scale and averaged over the 8 years considered are 0.28, 1.71, and 4.30 for the Majie Station, Danfeng Station, and Jingziguan Station, respectively. Additionally, the mean standard deviation of three products computed at the daily time scale are 0.21, 0.87, and 1.62, respectively.

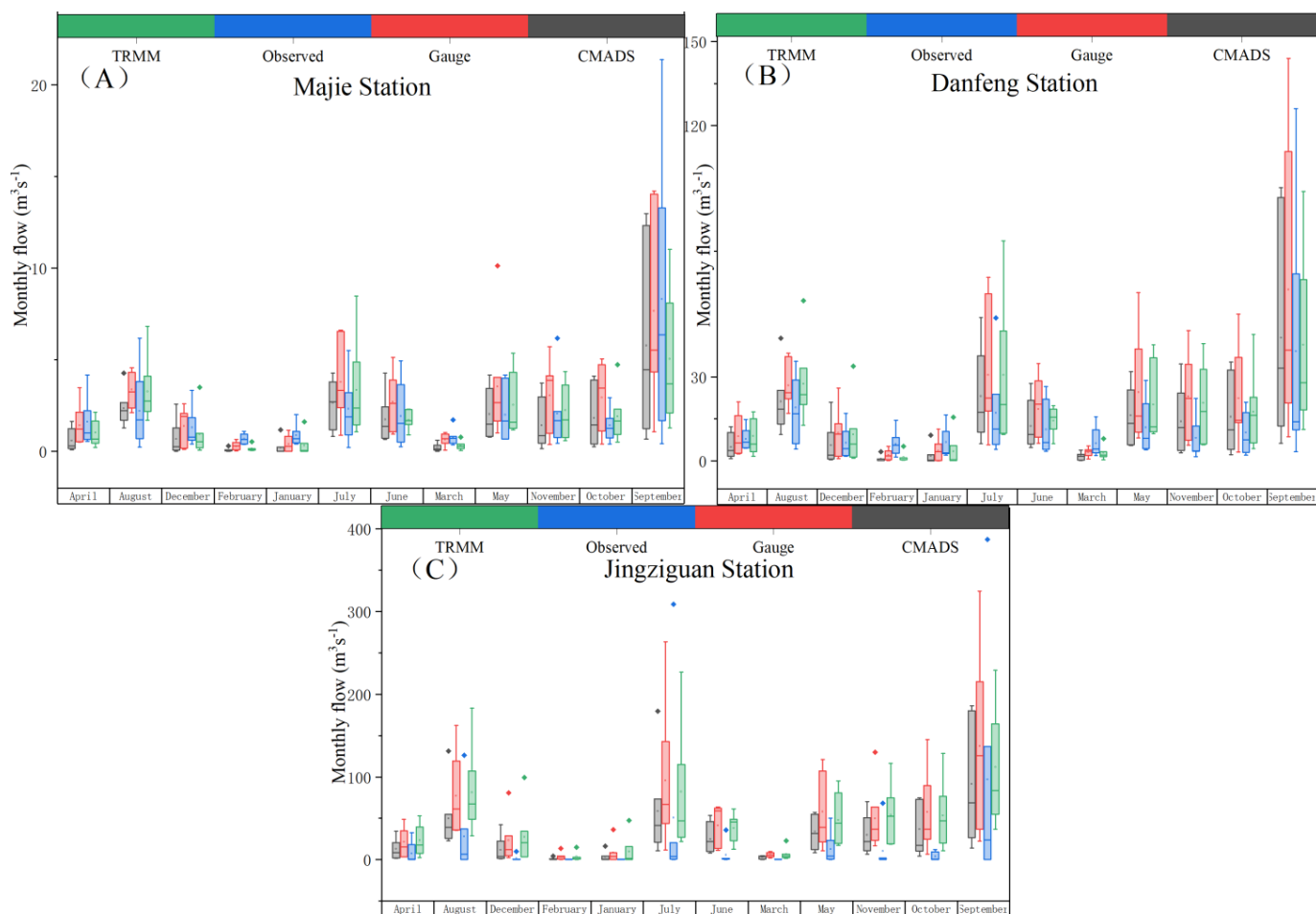


Figure 7. Box plot of the monthly runoff from 2006 to 2015, observed data and simulated stream-flow using CMADS, TRMM, and Gauge data at (A) Majie Station, (B) Danfeng Station, and (C) Jingziguan Station.

3.2.2. Post-Calibration Model Results

Seventeen parameters related to the hydrological process were selected to calibrate the SWAT model and the range of the parameters, as well as the result of the calibration, which are shown in Table 6. Be aware that the streamflow of Majie Station, Danfeng Station, and Jingziguan Station were calibrated together.

It is noted from Figure 8 that there is a positive correlation between the simulated runoff and rainfall. Moreover, the runoff of the CMADS model had a positive correlation with the measured runoff, but the smaller flood peaks were not simulated in the year when extreme flood events occurred or flood events were relatively continuous. The runoff trend of the TRMM model was similar to the measured runoff in the upper and lower reaches, but several consecutive flood events were simulated as a larger one in the middle stream. Though the runoff of the Gauge model was positively correlated with measured runoff in the upper stream, large floods in certain months were simulated as several smaller flood events in the midstream and downstream.

It is also noted from Table 7 that the R^2 values of the CMADS-SWAT (SWAT model derived from CMADS) and TRMM-SWAT were above 0.8 in the whole basin, except for the R^2 of the TRMM-SWAT in the middle reaches, which was 0.77. The NSE values of the CMADS-SWAT and TRMM-SWAT were all close to 0.8. However, the R^2 and NSE values of Gauge-SWAT were all below 0.6 in the whole basin and its R^2 and NSE values were only greater than 0.5 in the upstream. This suggested that the performances of CMADS-SWAT and TRMM-SWAT were better, while the performance of Gauge-SWAT was unsatisfactory.

Moreover, the PBIAS values of CMADS-SWAT and TRMM-SWAT were both greater than 25% in the upper and lower reaches and the PBIAS values in the middle stream were 9.9% and 0.0%, respectively, indicating that the CMADS-SWAT and TRMM-SWAT severely overestimated the runoff in the upper reach, severely underestimated the runoff in the downstream, and slightly overestimated the runoff in the middle reach. The PBIAS values of the Gauge-SWAT were both smaller than 15% in the middle and upper reaches and the PBIAS in the downstream was -89.3 , showing that the simulation values in the upper and middle reaches were higher and the simulation value was severely low in the downstream.

Table 6. Hydrological parameters chosen to calibrate the model (r_ and v_ mean a relative change and a replacement to the initial parameter values, respectively).

Parameters	Description	Monthly Scale			Daily Scale		
		CMADS	Gauge	TRMM	CMADS	Gauge	TRMM
r_SOL_AWC().sol	Available water capacity of the soil layer (mm HzO/mm soil)	−0.06	−0.26	−0.06	0.52	−0.76	−0.22
r_CN2.mgt	scS runoff curve number	0.14	−0.04	0.17	−0.21	−0.03	0.32
v_ALPHA_BF.gw	Baseflow alpha factor (days)	0.6	0.98	0.51	1.01	1.04	0.62
v_GW_DELAY.gw	Groundwater delay (days)	−139.76	234.5	−198.89	−216.84	209.46	481.86
r_GWQMN.gw	Threshold depth of water in the shallow aquifer required for return	−0.07	0.46	−0.64	−0.11	2.01	0.21
v_CH_K2.rte	Effective hydraulic conductivity (mm/h)	−367.12	175.49	−12.96	232.1	249.42	131.99
v_CH_N2.rte	Manning’s n value for main channel	0	0.04	0.13	0.03	0.15	0.13
v_REVAPMN.gw	Threshold depth of water in the shallow aquifer for “revamp” to occur	81.71	326.5	421.85	387.87	481.2	571.41
r_GW_REVAP.gw	Groundwater “revap” coefficient	−0.39	−0.38	−0.23	0.44	−0.34	0.21
r_OV_N.hru	Manning’s “n” value for overland flow	0.32	0.05	0.39	0.21	0.06	−1.11
r_SLSUBBSN.hru	Average slope length (m)	0.9	0.45	1.12	0.84	0.7	−0.52
r_HRU_SLP.hru	Average slope steepness (m/m)	−0.1	−0.38	−0.18	0.02	0.08	−0.47
v_EPCO.hru	Plant uptake compensation factor	0.34	0.59	−0.47	0.07	0.26	0.43
v_ESCO.hru	Soil evaporation compensation factor	0.15	0.05	0.02	0.89	0.15	0.37
r_SOL_BD().sol	Moist bulk density (g/cm ³)	2.19	1.5	1.22	1.31	1.79	1.64
r_SOL_K().sol	Saturated hydraulic conductivity (mm/h)	−0.55	−0.35	−0.56	−0.68	−0.75	−0.98
v_PLAPS.sub	Precipitation lapse rate (mm)	−716.86	690	−368.75	−867.07	615.05	−660.12

In summary, the performances of the CMADS model and TRMM model in the DRB were satisfactory across the sub-basins, but the performance of the Gauge-SWAT was only satisfactory in the upstream, deviating significantly from the observed data in the middle stream and downstream.

As was shown in Figure 9, though the CMADS and TRMM inputs replicated the runoff successfully at a daily scale, some small flood peaks were not simulated and the discharge of extreme floods during the flood season was significantly underestimated. The runoff of the Gauge model was notably different from the measured records and most of the floods were not simulated by the Gauge model.

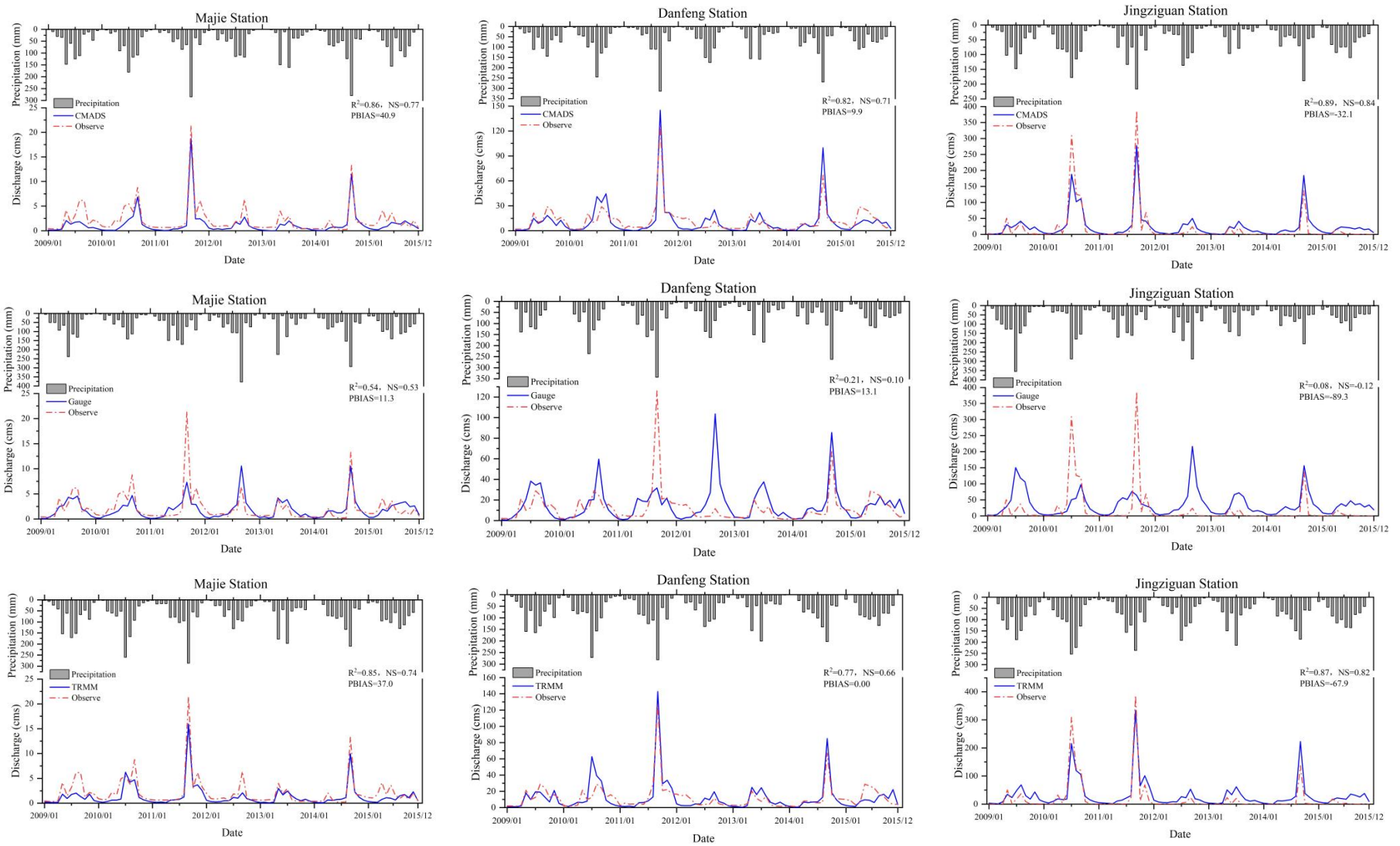


Figure 8. Observed and simulated discharges at Majie Station, Danfeng Station, and Jingziguan Station in the DRB at a monthly scale using inputs from Gauge, CMADS, and TRMM. Note that this figure is given as year/month.

Table 7. The post-calibration performance error amounts of the SWAT model simulated with CMADS, TRMM, and Gauge data on a monthly scale.

Station	R ²			NSE			PBIAS		
	CMADS	Gauge	TRMM	CMADS	Gauge	TRMM	CMADS	Gauge	TRMM
Majie Station	0.86	0.54	0.85	0.77	0.53	0.74	40.09	11.3	37
Danfeng Station	0.82	0.21	0.77	0.71	0.1	0.66	9.9	13.1	0
Jingziguan Station	0.89	0.08	0.87	0.84	0.12	0.82	−32.1	−89.3	−67.9

Specifically, according to Table 8, the CMADS-SWAT was the most successful in estimating runoffs because its R² and NSE values in the upstream and middle stream were all above 0.5, while its R² and NSE values were 0.42 and 0.34 in the downstream. The R² and NSE values of the TRMM-SWAT in the upper and lower reaches were all below 0.5, with the exception of that in the midstream, which was above 0.5, showing that the TRMM-SWAT underperformed in the upstream and downstream. Different from the CMADS-SWAT and the TRMM-SWAT, the performance of the Gauge-SWAT was unsatisfactory in the whole basin, for its R² and NSE values were all below 0.5. In addition, the PBIAS values of the CMADS-SWAT and the Gauge-SWAT were above zero in the upstream, below zero in the middle stream, and below 0.5 in the downstream, indicating that the discharge values of the CMADS-SWAT and the Gauge-SWAT were overestimated in the upstream and underestimated in the middle and lower reaches, especially in the downstream. Furthermore, the PBIAS values of the TRMM-SWAT in the upper, middle, and lower reaches were 42.8%, 20.4%, and −59.7%, respectively, showing that the discharge values derived from TRMM-SWAT were too high in the upstream and too low in the downstream.

Table 8. The post-calibration performance error amounts of the SWAT model simulated with CMADS, TRMM, and Gauge data on a daily monthly scale.

Station	R ²			NSE			PBIAS		
	CMADS	Gauge	TRMM	CMADS	Gauge	TRMM	CMADS	Gauge	TRMM
Majie Station	0.59	0.35	0.49	0.51	0.33	0.45	20.3	10.6	42.8
Danfeng Station	0.52	0.1	0.54	0.52	0.07	0.52	−4.5	−12.9	−20.4
Jingziguan Station	0.42	0.03	0.53	0.34	0.05	0.49	−65.5	−86.9	−59.7

The results after calibration indicated that CMADS-SWAT was superior to the other two precipitation products in both monthly and daily runoff simulation with the highest R² and NSE and a similar hydrological process line to the observed runoff. However, it was unexpected that the performance of the Gauge-SWAT was the worst, although the simulated runoff and rainfall had the same trend as the other two products. Moreover, all the three products tended to overestimate the runoff in the upper and middle reaches and underestimate that in downstream at the monthly scale. When it comes to the daily scale, all these three products overestimated the streamflow in upstream and underestimated the runoff in the lower and middle streams.

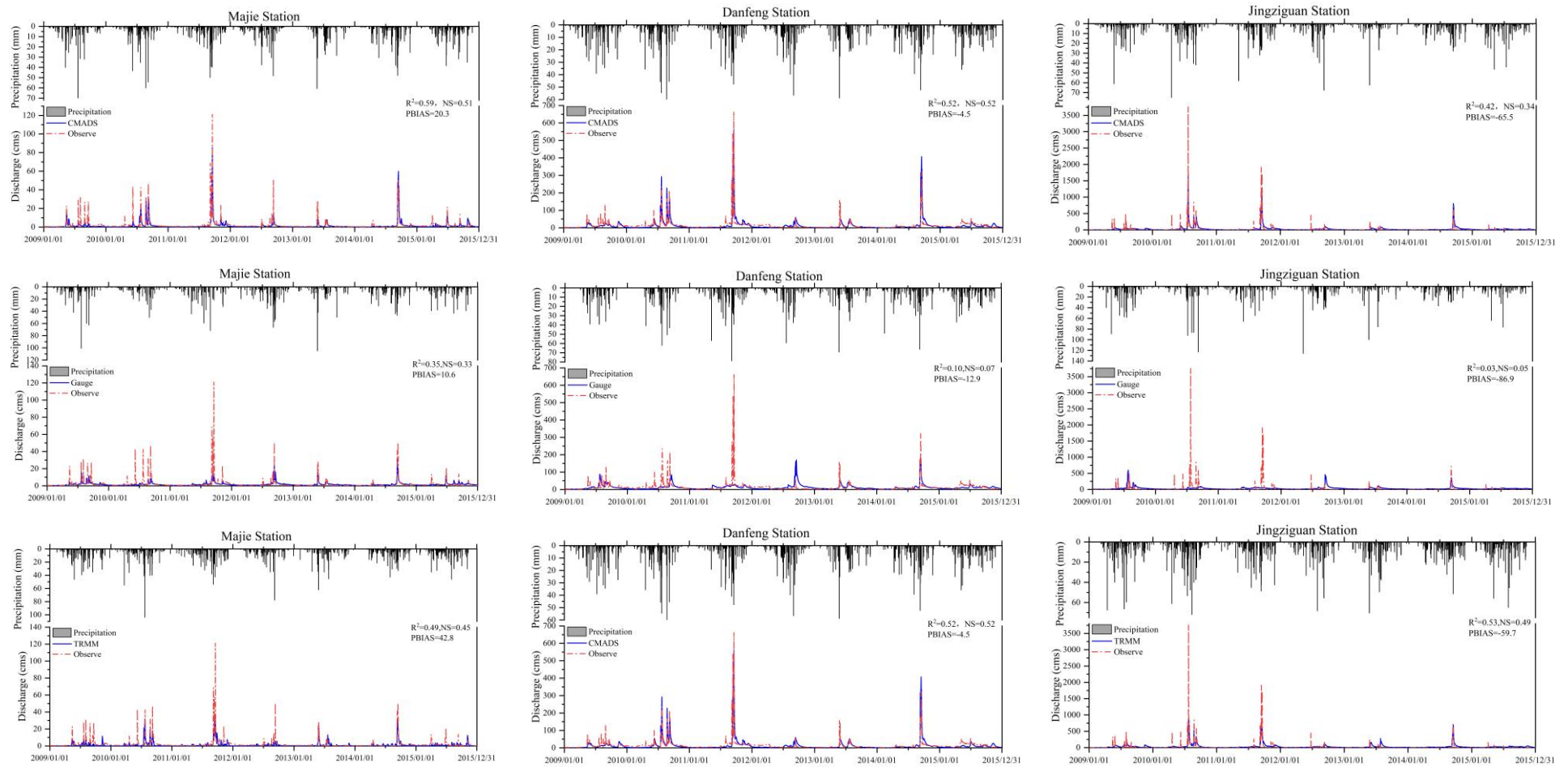


Figure 9. Observed and simulated discharges at Majie Station, Danfeng Station, and Jingziguan Station of the DRB at a daily scale using inputs of Gauge, CMADS, and TRMM. Note that this figure is given as year/month/day.

4. Discussion

Precipitation inputs play an important role in runoff simulation, and the errors can influence the accuracy of the hydrographical outputs [52]. Generally, precipitation inputs are evaluated on the basis of their predictable performances with hydrological parameters at the watershed scale, which avoids the scale difference found when using ground-based observations for validation [53]. This study evaluated the performance of RO and satellite-based precipitation datasets (CMADS and TRMM) in driving the SWAT model to simulate streamflow in the DRB on both monthly and daily scales. All modeling scenarios were calibrated and validated against runoff data measured at Majie Station, Danfeng Station, and Jingziguan Station. The SWAT-Cup's SUFI-2 algorithm was used for calibration and validation. Indices, including NSE, R^2 , and PBIAS, were selected to evaluate the efficiency of simulation runoff outcomes.

We found that compared with rainfall gauge observations, TRMM tended to underestimate the precipitation on both monthly and daily scales, while CMADS tended to overestimate the rainfall on the monthly scale but understate the rainfall on the daily scale. These findings are similar with previous studies. For example, Jiang et al. [21] found that TRMM underestimated precipitation on a daily scale in the Mishui Basin, Jiang et al. [47] found an average bias of -20.5% for CMADS over Xixian Basin, and Guo et al. [38] calculated an average bias of -28.7% for CMADS over Jinhua River Basin. The reason why CMADS underestimated the precipitation was the underestimation of the background field CMORPH data [54]. Additionally, the ability of TRMM and CMADS to identify the torrential rain events was worse than that of Gauge. In summary, the performance of CMADS in precipitation simulation was better than that of TRMM, maybe because the correct process of TRMM was simpler than that of CMADS [55]. The spatial distribution of the precipitation varied from dataset to dataset, namely, the rainfall of CMADS increased from the center to the surroundings and its rainfall in the central north was the highest. TRMM increased from upstream to downstream and the highest rainfall occurred in the east, but there is no obvious spatial distribution pattern with the rainfall of Gauge. This result can be explained by the different distributions of the rain gauge. In addition, all meteorological data were categorized into each sub-basin by the "nearest-distance" principle in the SWAT model [49], which contributed to the difference in the precipitation data from CMADS, TRMM, and Gauge as well. Moreover, the similarity between the rainfall of CMADS and Gauge was higher than that of the TRMM on both the monthly and daily scales, which is consistent with Wang's [56] research in the Ganjiang River Basin, where the area and elevation are similar to the DRB. Wang et al. [56] found that CMADS performed better than TRMM in precipitation estimation because of the different development processes of these two products. Only 500 stations were used to correct the TRMM data, while 2421 stations were used to correct the CMADS data [57,58]. Song et al. [59] conducted research on the Qujiang River Basin, ($38,900 \text{ km}^2$) finding that the spatial distribution of CMADS and TRMM was different from that of Gauge, which is consistent with our study.

Pre-calibration results showed that CMADS and TRMM were reliable enough to estimate runoffs on the monthly scale at Majie Station and Jingziguan Station, while they performed unsatisfactorily in simulating streamflow at Danfeng Station. The performances of Gauge in estimating runoff on the monthly scale in the middle stream and downstream were both unreliable, and only its performances in runoff simulation at the Majie Station was satisfactory. The performances of that on the daily scale, however, were all unsatisfactory. Moreover, all three datasets seriously overestimated the runoff in the middle stream and downstream on the monthly scale. Moreover, underestimation is probably better attributed to poor representation of the spatial variability of precipitation patterns in the middle and downstream, thereby causing the low ratio of streamflow to precipitation. According to Vu et al.'s [60] research, the underestimation can be attributed to the spatiotemporal uncertainty of the precipitation inputs. Previous studies indicated that the spatiotemporal uncertainty of the catchment rainfall was one of the main sources of uncertainty in runoff simulation using rainfall–runoff models [61–63]. Additionally, satellite-based precipitation

estimations have their own uncertainties [13]. This means that the satellite-based rainfall estimation affects the runoff simulation significantly [64]. Moreover, Rivera's research [65] found that previous conditions were more important before extreme floods, while previous conditions had little effect on conditions after extreme floods. It explains the result that the average observed streamflow was lower than the average simulated runoff and the average measured runoff was higher than the average observed runoff throughout the year in the upstream, except for September, because the underestimation in September in the Majie Station is the continuous precipitation before an extreme flood occurred in September.

When it comes to the post-calibration results, all three products tended to overestimate the runoff in the upper and middle reaches and underestimate the downstream at the monthly scale, while all three products overestimate the streamflow upstream and underestimate the runoff in the lower and middle streams at the daily scale. The overestimation at the monthly scale and the underestimation at the daily scale may be due to the overall inaccurate estimation of precipitation with the CMADS and TRMM data. In most cases, RO performed better than satellite precipitation in runoff simulation, even in sparsely gauged areas, when SWAT was used for modeling both monthly and daily scales, such as Vu et al.'s [60] research. Namely, they tested the accuracy of four satellite precipitation products, including TRMM 3B42 V7, PERSIANN, PERSIANN-Climate Data Record (PERSIANN-CDR), and CMADS, by using these four products to drive the SWAT model and comparing the runoff simulation results with the runoff simulated by gauged rainfall data in the Han River Basin in South Korea. Their results illustrated that the application of TRMM and CMADS in runoff simulation was worse than that of the gauges. However, our results vary from theirs. It is found in this paper that CMADS-SWAT was superior to the other two precipitation products in both monthly and daily runoff simulations, but Gauge-SWAT performed the worst in both monthly and daily streamflow simulations. This finding is not uncommon; for example, Song et al.'s [59] research on the Qujiang River Basin (38,900 km²) proved that the CMADS-SWAT performed best in the whole basin, followed by TRMM-SWAT and Gauge-SWAT, which performed the worst. That was mainly because of the non-uniform distribution of the gauges. According to Wang et al.'s [66] research, when the number of the stations is similar, the more uniform distribution of rainfall stations, the greater the NSE. In this study, the distribution of the Gauge was the most nonuniform, causing the performance of Gauge-SWAT to be the least satisfactory among the three products. Moreover, the gauge data only represent the observed rainfall at a specific station, whereas the CMADS and TRMM data represent precipitation averages over a large area [67]. For the variation of the topography that causes the precipitation variations over a short distance, the heterogeneity of the landscape of the weather forecasts by CMADS and TRMM is better. In addition, CMADS is a combination of the gauge and satellite data; therefore, its accuracy is higher than that of Gauge and TRMM.

At present, few studies have compared the performance of CMADS and TRMM data by using the SWAT model, because CMADS only covers East Asia and is a newly released dataset. Additionally, most studies are focused on evaluating the performance of CMADS, CHPRS, and CPC data or only studying the applicability of CFSR data by using the SWAT model [35,68]. Using different models or inputting different parameters will cause different results [69]. Therefore, the satellite or satellite-based products (including CMADS and TRMM) can be applied to the SWAT model or other models in the future to ensure that their replications of runoff are accurate and their predictions of rainfall are credible. Nonetheless, the datasets evaluated in this study can serve as viable alternatives in watersheds similar to the DRB where the observed precipitation data are unavailable.

5. Conclusions

In this study, CMADS and TRMM were evaluated on the basis of the measured records of the DRB using the SWAT model, and the main conclusions are as follows:

- (1) On the monthly scale, the precipitation measurements of CMADS and TRMM are similar to the rain gauge data. However, the rainfall data derived from TRMM and

CMADS have a different pattern from the precipitation of Gauge at the daily scale. Both TRMM and CMADS underestimate the precipitation, especially TRMM data. Moreover, the ability of CMADS and TRMM to simulate extreme precipitation (e.g., torrential rain) is worse than that of Gauge. The CMADS and TRMM data are also different from the Gauge data on the spatial scale. The rainfall data derived from CMADS tend to increase from the middle to the surroundings and the rainfall data derived from TRMM tend to decrease from upstream to downstream, while the precipitation of Gauge has no clear pattern.

- (2) The performance of CMADS-SWAT and TRMM-SWAT is consistent with the observed data from upstream to downstream at a monthly scale, while they both underestimate the runoff. However, Gauge-SWAT only performs satisfactorily in the upstream and its performance in the midstream and downstream is unsatisfactory. The ability of Gauge-SWAT to simulate extreme floods is poor, and the runoff is underestimated by Gauge-SWAT as well. However, only CMADS-SWAT performs satisfactorily in the whole basin at a daily scale, while both TRMM-SWAT and Gauge-SWAT performed unsatisfactorily in the middle and lower reaches. CMADS-SWAT, TRMM-SWAT, and Gauge-SWAT have all underestimated the runoff at a daily scale.
- (3) Among the three precipitation products, the performance of CMADS-SWAT is the best, followed by TRMM-SWAT. Gauge-SWAT had the worst performance, whether on the monthly scale or the daily scale.

Author Contributions: Conceptualization, Y.G. and W.D.; Y.G. and W.D.; software, Y.G.; validation, W.X. and X.Z.; formal analysis, Y.G.; investigation, Y.G.; resources, Y.G.; data curation, Y.G.; writing—original draft preparation, Y.G.; writing—review and editing, W.X., X.Z., W.T and X.W.; visualization, W.D.; supervision, W.D.; project administration, W.D.; funding acquisition, W.D. and W.T. All authors have read and agreed to the published version of the manuscript.

Funding: This research was funded by the National Key R&D Program of China (2021YFE0111900, 2019YFC1510705-05) and the National Natural Science Foundation of China (No.52109002). This paper was also funded by the basic scientific research business fee of scientific research institutes of the Changjiang Academy of Sciences, grant number CKSF2019185/TB.

Institutional Review Board Statement: Not applicable.

Informed Consent Statement: Not applicable.

Data Availability Statement: Not applicable.

Acknowledgments: We thank the editor and reviewers for their useful feedback that improved this paper. This study was supported by the National Key R&D Program of China (No. 2021YFE0111900, No. 2019YFC1510705-05), the National Natural Science Foundation of China (No.52109002), and the basic scientific research business fee of scientific research institutes of Changjiang Academy of Sciences (CKSF2019185/TB).

Conflicts of Interest: The authors declare no conflict of interest.

References

1. Lobligeois, F.; Andréassian, V.; Perrin, C.; Tabary, P.; Loumagne, C. When does higher spatial resolution rainfall information improve streamflow simulation: An evaluation using 3620 flood events. *Hydrol. Earth Syst. Sci.* **2014**, *18*, 575–594. [[CrossRef](#)]
2. Galván, L.; Olías, M.; Izquierdo, T.; Cerón, J.C.; Fernández de Villarán, R. Rainfall estimation in SWAT: An alternative method to simulate orographic precipitation. *J. Hydrol.* **2014**, *509*, 257–265. [[CrossRef](#)]
3. Roth, V.; Lemann, T. Comparing CFSR and conventional weather data for discharge and sediment loss modelling with SWAT in small catchments in the Ethiopian Highlands. *Hydrol. Earth Syst. Sci. Discuss.* **2015**, *12*, 2113–2153. [[CrossRef](#)]
4. Cornelissen, T.; Diekkrüger, B.; Bogena, H.R. Using high-resolution data to test parameter sensitivity of the distributed hydrological model HydroGeoSphere. *Water* **2016**, *8*, 202. [[CrossRef](#)]
5. Mileham, L.; Taylor, R.; Thompson, J.; Todd, M.; Tindimugaya, C. Impact of rainfall distribution on the parameterisation of a soil-moisture balance model of groundwater recharge in equatorial Africa. *J. Hydrol.* **2008**, *359*, 46–58. [[CrossRef](#)]
6. Remesan, R.; Holman, I.P. Effect of baseline meteorological data selection on hydrological modelling of climate change scenarios. *J. Hydrol.* **2015**, *528*, 631–642. [[CrossRef](#)]

7. Bohnenstengel, S.I.; Schlünzen, K.H.; Beyrich, F. Representativity of in situ precipitation measurements – A case study for the LITFASS area in North-Eastern Germany. *J. Hydrol.* **2011**, *400*, 387–395. [[CrossRef](#)]
8. Liu, J.; Kummerow, C.D.; Elsaesser, G.S. Identifying and analysing uncertainty structures in the TRMM microwave imager precipitation product over tropical ocean basins. *Int. J. Remote Sens.* **2016**, *38*, 23–42. [[CrossRef](#)]
9. Zhu, H.; Li, Y.; Liu, Z.; Shi, X.; Fu, B.; Xing, Z. Using SWAT to simulate streamflow in Huifa River basin with ground and Fengyun precipitation data. *J. Hydroinf.* **2015**, *17*, 834–844. [[CrossRef](#)]
10. Musie, M.; Sen, S.; Srivastava, P. Comparison and evaluation of gridded precipitation datasets for streamflow simulation in data scarce watersheds of Ethiopia. *J. Hydrol.* **2019**, *579*, 124168. [[CrossRef](#)]
11. Belete, M.; Deng, J.; Wang, K.; Zhou, M.; Zhu, E.; Shifaw, E.; Bayissa, Y. Evaluation of satellite rainfall products for modeling water yield over the source region of Blue Nile Basin. *Sci. Total Environ.* **2020**, *708*, 134834. [[CrossRef](#)] [[PubMed](#)]
12. Oreggioni Weiberlen, F.; Báez Benítez, J. Assessment of satellite-based precipitation estimates over Paraguay. *Acta Geophys.* **2018**, *66*, 369–379. [[CrossRef](#)]
13. Duan, Z.; Liu, J.; Tuo, Y.; Chiogna, G.; Disse, M. Evaluation of eight high spatial resolution gridded precipitation products in Adige Basin (Italy) at multiple temporal and spatial scales. *Sci. Total Environ.* **2016**, *573*, 1536–1553. [[CrossRef](#)]
14. Luo, X.; Wu, W.; He, D.; Li, Y.; Ji, X. Hydrological Simulation Using TRMM and CHIRPS Precipitation Estimates in the Lower Lancang-Mekong River Basin. *Chinese Geogr. Sci.* **2019**, *29*, 13–25. [[CrossRef](#)]
15. Cecinati, F.; Moreno-Ródenas, A.M.; Rico-Ramirez, M.A.; ten Veldhuis, M.C.; Langeveld, J.G. Considering Rain Gauge Uncertainty Using Kriging for Uncertain Data. *Atmosphere* **2018**, *9*, 446. [[CrossRef](#)]
16. Peleg, N.; Ben-Asher, M.; Morin, E. Radar subpixel-scale rainfall variability and uncertainty: Lessons learned from observations of a dense rain-gauge network. *Hydrol. Earth Syst. Sci.* **2013**, *17*, 2195–2208. [[CrossRef](#)]
17. Hwang, Y.; Clark, M.P.; Rajagopalan, B. Use of daily precipitation uncertainties in streamflow simulation and forecast. *Stoch. Environ. Res. Risk Assess.* **2011**, *25*, 957–972. [[CrossRef](#)]
18. Alijanian, M.; Rakhshandehroo, G.R.; Mishra, A.K.; Dehghani, M. Evaluation of satellite rainfall climatology using CMORPH, PERSIANN-CDR, PERSIANN, TRMM, MSWEP over Iran. *Int. J. Climatol.* **2017**, *37*, 4896–4914. [[CrossRef](#)]
19. Sun, Q.; Miao, C.; Duan, Q.; Ashouri, H.; Sorooshian, S.; Hsu, K.L. A Review of Global Precipitation Data Sets: Data Sources, Estimation, and Intercomparisons. *Rev. Geophys.* **2018**, *56*, 79–107. [[CrossRef](#)]
20. Hur, J.; Raghavan, S.V.; Nguyen, N.S.; Liong, S.Y. Evaluation of High-resolution Satellite Rainfall Data over Singapore. *Procedia Eng.* **2016**, *154*, 158–167. [[CrossRef](#)]
21. Jiang, S.; Ren, L.; Hong, Y.; Yang, X.; Ma, M.; Zhang, Y.; Yuan, F. Improvement of Multi-Satellite Real-Time Precipitation Products for Ensemble Streamflow Simulation in a Middle Latitude Basin in South China. *Water Resour. Manag.* **2014**, *28*, 2259–2278. [[CrossRef](#)]
22. Duncan, J.M.A.; Biggs, E.M. Assessing the accuracy and applied use of satellite-derived precipitation estimates over Nepal. *Appl. Geogr.* **2012**, *34*, 626–638. [[CrossRef](#)]
23. Yan, R.; Gao, J.; Huang, J. WALRUS-paddy model for simulating the hydrological processes of lowland polders with paddy fields and pumping stations. *Agric. Water Manag.* **2016**, *169*, 148–161. [[CrossRef](#)]
24. Gokhan Yilmaz, A.; Alam Imteaz, M.; Ogwuda, O. Accuracy of HEC-HMS and LBRM Models in Simulating Snow Runoffs in Upper Euphrates Basin. *J. Hydrol. Eng.* **2011**, *17*, 342–347. [[CrossRef](#)]
25. Wu, J.; Chen, X.; Yu, Z.; Yao, H.; Li, W.; Zhang, D. Assessing the impact of human regulations on hydrological drought development and recovery based on a ‘simulated-observed’ comparison of the SWAT model. *J. Hydrol.* **2019**, *577*, 123990. [[CrossRef](#)]
26. Bhuiyan, M.A.E.; Nikolopoulos, E.I.; Anagnostou, E.N.; Polcher, J.; Albergel, C.; Dutra, E.; Fink, G.; Martínez-De La Torre, A.; Munier, S. Assessment of precipitation error propagation in multi-model global water resource reanalysis. *Hydrol. Earth Syst. Sci.* **2019**, *23*, 1973–1994. [[CrossRef](#)]
27. Solakian, J.; Maggioni, V.; Lodhi, A.; Godrej, A. Investigating the use of satellite-based precipitation products for monitoring water quality in the Occoquan Watershed. *J. Hydrol. Reg. Stud.* **2019**, *26*, 100630. [[CrossRef](#)]
28. Price, K.; Purucker, S.T.; Kraemer, S.R.; Babendreier, J.E.; Knightes, C.D. Comparison of radar and gauge precipitation data in watershed models across varying spatial and temporal scales. *Hydrol. Process.* **2014**, *28*, 3505–3520. [[CrossRef](#)]
29. Wang, H.; Sun, F.; Xia, J.; Liu, W. Impact of LUCC on streamflow based on the SWAT model over the Wei River basin on the Loess Plateau in China. *Hydrol. Earth Syst. Sci.* **2017**, *21*, 1929–1945. [[CrossRef](#)]
30. Qiu, J.; Yang, Q.; Zhang, X.; Huang, M.; Adam, J.C.; Malek, K. Implications of water management representations for watershed hydrologic modeling in the Yakima River basin. *Hydrol. Earth Syst. Sci.* **2019**, *23*, 35–49. [[CrossRef](#)]
31. Li, D.; Christakos, G.; Ding, X.; Wu, J. Adequacy of TRMM satellite rainfall data in driving the SWAT modeling of Tiaoxi catchment (Taihu lake basin, China). *J. Hydrol.* **2018**, *556*, 1139–1152. [[CrossRef](#)]
32. Huang, Y.; Bárdossy, A.; Zhang, K. Sensitivity of hydrological models to temporal and spatial resolutions of rainfall data. *Hydrol. Earth Syst. Sci.* **2019**, *23*, 2647–2663. [[CrossRef](#)]
33. Dhanesh, Y.; Bindhu, V.M.; Senent-Aparicio, J.; Brighenti, T.M.; Ayana, E.; Smitha, P.S.; Fei, C.; Srinivasan, R. A Comparative Evaluation of the Performance of CHIRPS and CFSR Data for Different Climate Zones Using the SWAT Model. *Remote Sens.* **2020**, *12*, 3088. [[CrossRef](#)]

34. Al-Falahi, A.H.; Saddique, N.; Spank, U.; Gebrechorkos, S.H.; Bernhofer, C. Evaluation the performance of several gridded precipitation products over the highland region of yemen for water resources management. *Remote Sens.* **2020**, *12*, 2984. [[CrossRef](#)]
35. Mararakanye, N.; Le Roux, J.J.; Franke, A.C. Using satellite-based weather data as input to SWAT in a data poor catchment. *Phys. Chem. Earth, Parts A/B/C* **2020**, *117*, 102871. [[CrossRef](#)]
36. Dao, D.M.; Lu, J.; Chen, X.; Kantoush, S.A.; Van Binh, D.; Phan, P.; Tung, N.X. Predicting tropical monsoon hydrology using CFSR and CMADS data over the Cau river basin in Vietnam. *Water* **2021**, *13*, 1314. [[CrossRef](#)]
37. Gao, Z.; Long, D.; Tang, G.; Zeng, C.; Huang, J.; Hong, Y. Assessing the potential of satellite-based precipitation estimates for flood frequency analysis in ungauged or poorly gauged tributaries of China's Yangtze River basin. *J. Hydrol.* **2017**, *550*, 478–496. [[CrossRef](#)]
38. Guo, M.; Zhang, T.; Li, J.; Li, Z.; Xu, G.; Yang, R. Reducing nitrogen and phosphorus losses from different crop types in the water source area of the Danjiang river, China. *Int. J. Environ. Res. Public Health* **2019**, *16*, 3442. [[CrossRef](#)] [[PubMed](#)]
39. Gu, W.; Shao, D.; Jiang, Y. Risk Evaluation of Water Shortage in Source Area of Middle Route Project for South-to-North Water Transfer in China. *Water Resour. Manag.* **2012**, *26*, 3479–3493. [[CrossRef](#)]
40. Dong, Z.; Yan, Y.; Duan, J.; Fu, X.; Zhou, Q.; Huang, X.; Zhu, X.; Zhao, J. Computing payment for ecosystem services in watersheds: An analysis of the Middle Route Project of South-to-North Water Diversion in China. *J. Environ. Sci.* **2011**, *23*, 2005–2012. [[CrossRef](#)]
41. Hu, S.; Qiu, H.; Yang, D.; Cao, M.; Song, J.; Wu, J.; Huang, C.; Gao, Y. Evaluation of the applicability of climate forecast system reanalysis weather data for hydrologic simulation: A case study in the Bahe River Basin of the Qinling Mountains, China. *J. Geogr. Sci.* **2017**, *27*, 546–564. [[CrossRef](#)]
42. Shan, Z.B.Z.Z.R. The Impact of Land Use and Agricultural Management on Non-point Source Nitrogen Pollution in Dan River Watershed. *J. Soil Water Conserv.* **2020**, *34*, 135–141.
43. Meng, X.; Sun, Z.; Zhao, H.; Ji, X.; Wang, H.; Xue, L.; Wu, H.; Zhu, Y. Spring flood forecasting based on the WRF-TSRM mode. *Teh. Vjesn.* **2018**, *25*, 141–151. [[CrossRef](#)]
44. Meng, X.; Wang, H.; Wu, Y.; Long, A.; Wang, J.; Shi, C.; Ji, X. Investigating spatiotemporal changes of the land-surface processes in Xinjiang using high-resolution CLM3.5 and CLDAS: Soil temperature. *Sci. Rep.* **2017**, *7*, 1–14. [[CrossRef](#)] [[PubMed](#)]
45. Keikhosravi Kiany, M.S.; Masoodian, S.A.; Balling, R.C.; Montazeri, M. Evaluation of the TRMM 3B42 product for extreme precipitation analysis over southwestern Iran. *Adv. Sp. Res.* **2020**, *66*, 2094–2112. [[CrossRef](#)]
46. Huffman, G.J.; Adler, R.F.; Bolvin, D.T.; Nelkin, E.J. The TRMM Multi-Satellite Precipitation Analysis (TMPA). *Satell. Rainfall Appl. Surf. Hydrol.* **2010**, 3–22. [[CrossRef](#)]
47. Jiang, S.; Liu, R.; Ren, L.; Wang, M.; Shi, J.; Zhong, F.; Duan, Z. Evaluation and Hydrological Application of CMADS Reanalysis Precipitation Data against Four Satellite Precipitation Products in the Upper Huaihe River Basin, China. *J. Meteorol. Res.* **2020**, *34*, 1096–1113. [[CrossRef](#)]
48. Duan, Z.; Tuo, Y.; Liu, J.; Gao, H.; Song, X.; Zhang, Z.; Yang, L.; Mekonnen, D.F. Hydrological evaluation of open-access precipitation and air temperature datasets using SWAT in a poorly gauged basin in Ethiopia. *J. Hydrol.* **2019**, *569*, 612–626. [[CrossRef](#)]
49. Pang, J.; Zhang, H.; Xu, Q.; Wang, Y.; Wang, Y.; Zhang, O.; Hao, J. Hydrological evaluation of open-access precipitation data using SWAT at multiple temporal and spatial scales. *Hydrol. Earth Syst. Sci.* **2020**, *24*, 3603–3626. [[CrossRef](#)]
50. Zhang, B.; Xu, X.; Liu, W.; Chen, T. Dynamic changes of soil moisture in loess hilly and gully region under effects of different yearly precipitation patterns. *Chinese J. Appl. Ecol.* **2008**, *19*, 1234–1240.
51. Azarnivand, A.; Camporese, M.; Alaghmand, S.; Daly, E. Simulated response of an intermittent stream to rainfall frequency patterns. *Hydrol. Process.* **2020**, *34*, 615–632. [[CrossRef](#)]
52. Knoche, M.; Fischer, C.; Pohl, E.; Krause, P.; Merz, R. Combined uncertainty of hydrological model complexity and satellite-based forcing data evaluated in two data-scarce semi-arid catchments in Ethiopia. *J. Hydrol.* **2014**, *519*, 2049–2066. [[CrossRef](#)]
53. Bai, P.; Liu, X. Evaluation of Five Satellite-Based Precipitation Products in Two Gauge-Scarce Basins on the Tibetan Plateau. *Remote Sens.* **2018**, *10*, 1316. [[CrossRef](#)]
54. Zhou, Z.; Gao, X.; Yang, Z.; Feng, J.; Meng, C.; Xu, Z. Evaluation of hydrological application of CMADS in Jinhua River Basin, China. *Water* **2019**, *11*, 138. [[CrossRef](#)]
55. Sun, R.; Yuan, H.; Liu, X.; Jiang, X. Evaluation of the latest satellite-gauge precipitation products and their hydrologic applications over the Huaihe River basin. *J. Hydrol.* **2016**, *536*, 302–319. [[CrossRef](#)]
56. Wang, Q.; Xia, J.; Zhang, X.; She, D.; Liu, J.; Li, P. Multi-scenario integration comparison of cmads and tmpa datasets for hydro-climatic simulation over ganjiang river basin, china. *Water* **2020**, *12*, 3243. [[CrossRef](#)]
57. Liu, S.; Yan, D.; Qin, T.; Weng, B.; Li, M. Correction of TRMM 3B42V7 Based on Linear Regression Models over China. *Adv. Meteorol.* **2016**, *2016*, 3103749. [[CrossRef](#)]
58. Chen, S.; Hong, Y.; Cao, Q.; Gourley, J.J.; Kirstetter, P.E.; Yong, B.; Tian, Y.; Zhang, Z.; Shen, Y.; Hu, J.; et al. Similarity and difference of the two successive V6 and V7 TRMM multisatellite precipitation analysis performance over China. *J. Geophys. Res. Atmos.* **2013**, *118*, 13060–13074. [[CrossRef](#)]
59. Song, Y.; Zhang, J.; Meng, X.; Zhou, Y.; Lai, Y.; Cao, Y. Comparison study of multiple precipitation forcing data on hydrological modeling and projection in the qujiang river basin. *Water* **2020**, *12*, 2626. [[CrossRef](#)]

60. Vu, T.T.; Li, L.; Jun, K.S. Evaluation of multi-satellite precipitation products for streamflow simulations: A case study for the Han River Basin in the Korean Peninsula, East Asia. *Water* **2018**, *10*, 642. [[CrossRef](#)]
61. Hromadka, T.V.; McCuen, R.H. Uncertainty estimates for surface runoff models. *Adv. Water Resour.* **1988**, *11*, 2–14. [[CrossRef](#)]
62. Maskey, S.; Guinot, V.; Price, R.K. Treatment of precipitation uncertainty in rainfall-runoff modelling: A fuzzy set approach. *Adv. Water Resour.* **2004**, *27*, 889–898. [[CrossRef](#)]
63. Jones, P.D.; Lister, D.H.; Wilby, R.L.; Kostopoulou, E. Extended riverflow reconstructions for England and Wales, 1865-2002. *Int. J. Climatol.* **2006**, *26*, 219–231. [[CrossRef](#)]
64. Andréassian, V.; Perrin, C.; Michel, C.; Usart-Sanchez, I.; Lavabre, J. Impact of imperfect rainfall knowledge on the efficiency and the parameters of watershed models. *J. Hydrol.* **2001**, *250*, 206–223. [[CrossRef](#)]
65. Solano-Rivera, V.; Geris, J.; Granados-Bolaños, S.; Brenes-Cambronero, L.; Artavia-Rodríguez, G.; Sánchez-Murillo, R.; Birkel, C. Exploring extreme rainfall impacts on flow and turbidity dynamics in a steep, pristine and tropical volcanic catchment. *CATENA* **2019**, *182*, 104118. [[CrossRef](#)]
66. Xu, Q.W.Y.C.X.Z. Influence of Rain Gauges Network Configuration on the Accuracy of Rainfall Spatial Interpolation and Hydrological Modeling. *J. Yangtze River Sci. Res. Inst.* **2019**, *4*, 19–26.
67. Fuka, D.R.; Walter, M.T.; Macalister, C.; Degaetano, A.T.; Steenhuis, T.S.; Easton, Z.M. Using the Climate Forecast System Reanalysis as weather input data for watershed models. *Hydrol. Process.* **2014**, *28*, 5613–5623. [[CrossRef](#)]
68. Tuo, Y.; Duan, Z.; Disse, M.; Chiogna, G. Evaluation of precipitation input for SWAT modeling in Alpine catchment: A case study in the Adige river basin (Italy). *Sci. Total Environ.* **2016**, *573*, 66–82. [[CrossRef](#)] [[PubMed](#)]
69. Nash, J.E.; Sutcliffe, J.V. River flow forecasting through conceptual models part I — A discussion of principles. *J. Hydrol.* **1970**, *10*, 282–290. [[CrossRef](#)]